# Radiation Effect on the Thermal Conductivity and Diffusivity of Ramie Fibers in a Range of Low Temperatures by $\gamma$ Rays

**Atsuhiko Yamanaka,[1] Yoshinobu Izumi,[2] Takaya Terada,[2] Kimiko Ema,[2] Masayuki Tsutsumi,[1] Muneatsu Nakamura,[1] Takeshi Oohazama,[1] Tooru Kitagawa,[1] Hiroyuki Fujishiro,[3] Shunzo Abe,[1] Shigehiro Nishijima[2]**

[1]*Research Center, Toyobo Company, Limited, 2-1-1, Katata, Ohtsu, Shiga 520-0292, Japan*
[2]*Department of Nuclear Engineering, Graduate School of Engineering, Osaka University, Yamadaoka 2-1, Suita, Osaka 565-0871, Japan*
[3]*Department of Materials Science and Technology, Faculty of Engineering, Iwate University, Ueda 4-3-5, Morioka 020-8551, Japan*

Received 30 June 2005; accepted 3 October 2005
DOI 10.1002/app.23838
Published online in Wiley InterScience (www.interscience.wiley.com).

**ABSTRACT:** To understand the influence on the thermal conductivity by the length of the molecular chain in the polymer fiber, the thermal conductivity and thermal diffusivity of ramie fibers and those irradiated by $\gamma$ rays, which induced molecular chain scission of cellulose, were investigated in a range of low temperatures. The degrees of polymerization, crystallinities, and orientation angles of ramie fibers and those irradiated by $\gamma$ rays ($\gamma$-ray treatment) were measured by the solution viscosity method, solid-state NMR, and X-ray diffraction. Only the degree of polymerization decreased with the $\gamma$-ray treatment, and the crystallinities and orientation angles were almost independent of the $\gamma$-ray treatment. The thermal conductivities of the ramie fibers with and without $\gamma$-ray treatments decreased with decreasing temperature. The thermal diffusivities of the ramie fibers and those irradiated by $\gamma$ rays were almost constant from 250 to 100 K, increased slightly with the temperature decreasing from 100 to 50 K, and increased rapidly with the temperature decreasing below 50 K. The thermal conductivity and thermal diffusivity of the ramie fibers decreased with the $\gamma$-ray treatment. The mean free path of the phonon in the ramie fibers was reduced by the $\gamma$-ray treatment. This decrease of the thermal diffusivity and thermal conductivity was explained by the reduction of the mean free path of the phonon by molecular chain scission with $\gamma$ rays.  J Appl Polym Sci 100: 5007–5018, 2006

**Key words:** chain; fibers; radiation; thermal properties

## INTRODUCTION

Thermal conductivity is an important property in applications of polymeric materials, such as a cool/warm sensation for clothing fiber or wood products and the thermal insulation of plastics, including styroforms.[1–4] With the recent development of superconducting and electronic engineering technologies, the thermal conductivity of structural and insulating materials used as composites in cryogenic and heat-releasing materials in electrical equipment has become more important. Furthermore, the desired features vary, depending on the application, from insulation for use in cryostats[5] to high thermal conductivity for use in superconducting coils[6] and electronic engineering.[7] The investigation of the factors that affect the thermal conductivity of polymeric materials is essential to enable the formation of technologies for designing polymeric materials that possess the required thermal conductivity.

From previous studies of polymeric materials, it is well known that the thermal conductivity of amorphous polymers is smaller than that of metals and semiconductors.[8,9] Therefore, these have principally been used as heat insulators. However, other reports have shown that polymeric crystals possess a high thermal conductivity in the direction in which the molecular chains are covalently bonded, polyethylene crystals being an example.[10–17] The thermal conductivity of electrical insulators is considered to be attributable to phonons,[10,12] and the heat in polymers is conducted in the direction of covalently bonded molecular chains, whereas conduction in the direction to intermolecular chains bonded by van der Waals forces is much less. Therefore, the thermal conductivity depends on the crystallization, orientation, crystal size, and defects in the polymer crystal material. Thus, high-crystallization and high-orientation polymers exhibit high thermal conductivity.[11–17] For example,

*Correspondence to:* A. Yamanaka (Atsuhiko_Yamanaka@kt.toyobo.co.jp).

highly crystallized polymeric materials, including high-strength polyethylene fiber[11,17–19] and high-strength poly(*para*-phenylenebenzobisoxazole) fiber,[18] are known to possess high thermal conductivity similar to that of metals. The thermal conductivity of polymers, therefore, ranges from high to low, depending on the crystal structure or morphology.

The thermal conductivity of solid electrically insulating materials is affected by the scattering of phonons. The phonon scattering is considered to be introduced by imperfections on the surface of the material, the grain boundaries, or intracrystal or interphonon dispersion in the material.[20] Therefore, in polymers, the crystal or amorphous boundary, defects, ends, and entanglements of the molecular chains can scatter phonons and interfere with the thermal transmittance. Therefore, in the case of the thermal conduction of polymer fibers in the fiber direction, the mean free path of phonons is influenced not only by the crystallization or orientation but also by the length of molecular chains and the bridge structure. The changes in the mean free path of phonons result in changes in the thermal conductivity. In this report, the dependence of the thermal conductivity on the length of the molecular chain in the polymer fibers is described.

It is well known that fibers mainly made of cellulose, including ramie and cottons, undergo main-chain scission by irradiation with $\gamma$ rays.[21] It is also known that the crystallinity is not reduced by irradiation with $\gamma$ rays in the case of an appropriate dose rate.[21] In this article, we report the changes in the thermal conductivity and thermal diffusivity of ramie fibers by chain scission with the radiation of $\gamma$ rays.

## EXPERIMENTAL

### Sample

In this work, the thermal conductivity and diffusivity of ramie fibers and those irradiated with $\gamma$ rays ($\gamma$-ray treatment) were measured in a range of low temperatures. The sample preparations are described in the following.

#### Ramie fibers

The ramie fiber samples used in this work were made in China. The ramie fibers were scoured and bleached. The density and fineness of the ramie fibers were 1.54 g/cm$^3$ and 4.3 dtex, respectively.

#### Irradiation with $\gamma$ rays

The purpose of this work was the investigation of the relation between the thermal conductivity and length of the molecular chain. For this purpose, ramie fibers made of short molecular chains were prepared with chain scission in the ramie fibers by irradiation with $\gamma$ rays. Irradiation was carried out with Co-60 $\gamma$ rays at the Institute of Scientific and Industrial Research (Sanken) at Osaka University at the ambient temperature and in air. The absorbed dose rate and irradiation time were 0.5 kGy/h and 2 h, 1.0 kGy/h and 2 h, and 16.7 kGy/h and 6 h. The total absorbed doses were 1, 2, and 100 kGy, respectively. These are abbreviated to ramie (1 kGy), ramie (2 kGy), and ramie (100 kGy), respectively. The densities of the ramie fibers with $\gamma$-ray treatments were 1.54 g/cm$^3$. Those densities were measured by a pycnometer after drying at 383 K for 8 h.

### Characterization

The lengths of the molecular chains of ramie fibers with $\gamma$-ray treatments were measured by the degree of polymerization (DP). The DPs of ramie fibers with the $\gamma$-ray treatment for chain scission were measured by the solution viscosity method. The thermal conductivity and diffusivity depended on not only the length of the molecular chain, which was expected to influence the mean free path of the phonon, but also the changes in the crystallinity and orientation angle by the $\gamma$-ray treatment.[11–17] To clarify the changes in the ramie fibers, the crystallinities were measured by solid-state, high-resolution NMR, and the orientation angles were measured by X-ray diffraction. Those measurements are described in the following.

#### DP

DPs of the ramie fibers with and without the $\gamma$-ray treatment were measured by the viscosity method with a copper ethylene diamine (CED) solution, as shown in the following.[22,23] Copper hydroxide (II) was dissolved in a 4.5*N* ethylene diamine aqueous solution at a concentration of 55 g/500 mL. A CED solution was prepared via the stirring of this solution for 2 h at room temperature. The ramie fibers with and without $\gamma$-ray treatments were dissolved in the CED solution at a concentration of 0.008 g/25 mL, and those solutions were stirred for 30 min at room temperature. The relative viscosities ($t/t_0$) at 293 K of the sample solutions were measured with Ubbelohde viscometers in a thermostat. The DPs of the ramie fibers with and without the $\gamma$-ray treatment were estimated from the measured viscosities. The parameters $t$ and $t_0$ are defined as the dropping times of the CED solution with and without the dissolution of ramie fibers, respectively. The DPs of the ramie fibers were estimated by $t/t_0$.

#### Crystallinity

The crystal and amorphous parts have different chemical shifts of the C4 and C6 carbon peaks in the solid-

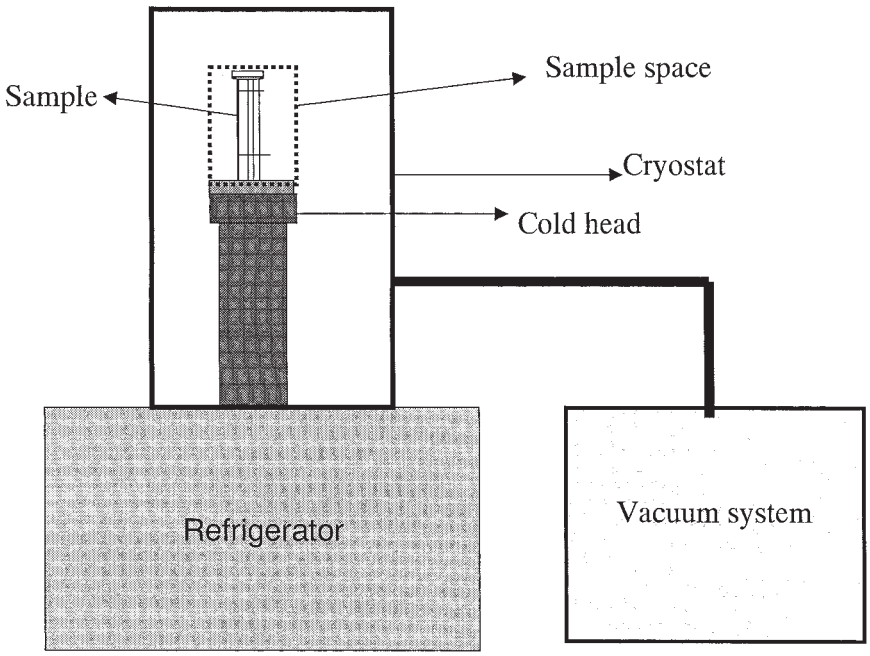


**Figure 1** Schematic diagram of the thermal conductivity and diffusivity measurement system.

state $^{13}$C-NMR spectrum of cellulose (e.g., ramie).[24–26] Therefore, it is possible to obtain the ratio of crystal and amorphous parts by peak separation in the NMR spectrum. It is also possible to study the molecular motions of the crystal and amorphous parts by the analysis of the relaxation time of the crystal and amorphous peaks in the NMR spectrum, respectively.[27,28] It is also known that the chemical shifts of cellulose in solid-state $^{13}$C-NMR spectra are different through the difference of the crystal structure (e.g., celluloses I and II).[24,25,29,30] The relations between the chemical shifts and torsion angles of the molecular chain in cellulose crystal have been reported.[26] The changes in the crystal structures and crystallinities of cellulose fibers by mercerization or a liquid ammonia treatment were studied by solid-state NMR.[31,32] In this work, the changes in the crystal structure and crystallinity by the $\gamma$-ray treatment were investigated with solid-state NMR. The crystallinities were estimated by the peak separation of the C4 carbon.

Solid-state NMR measurements were carried out on Bruker Avance 300 ($^{13}$C, 75.5 MHz) (Rheinstetten, Germany). NMR spectra were measured by the cross-polarization (CP), high-power proton decoupling, magic-angle-spinning (MAS) method. The pulse width was 4 $\mu$s, and the MAS rate was 4.5 kHz.

### Orientation angle

The orientation angle of the crystalline phase to the fiber axis was estimated by X-ray diffraction. The samples were prepared in the form of a bundle of about 30 filaments in parallel, and they were fixed at both ends. A Rigaku RU-200 (40 kV and 100 mA) (Akishima, Tokyo, Japan) was used with X-ray diffraction on Ni-filtered Cu K$\alpha$ ($\lambda$ = 0.1548 nm). The intensity distribution of the (002) diffraction spot was used for estimating the orientation angles.

## Measurements

In this work, the thermal conductivities and thermal diffusivities in the fiber direction of the ramie fibers prepared as shown in the previous section were measured. The tensile modulus of those ramie fibers with and without the $\gamma$-ray treatment were measured to investigate the contribution of the sound velocity to the thermal conductivity and diffusivity. The measurements of the thermal conductivity, thermal diffusivity, and tensile modulus are described in the following.

### Thermal conductivity

The thermal conductivity was measured by a steady-state heat flow method.[18,33] The measurements of the thermal conductivity were carried out on an automated measuring system with a thermal controller of a Gifford–MacMahon (GM) cycle helium refrigerator (Sumitomo Heavy Industries, Shinagawa, Tokyo, Japan) as a cryostat.[33] A schematic diagram of the thermal conductivity measurement system is shown in Figure 1.

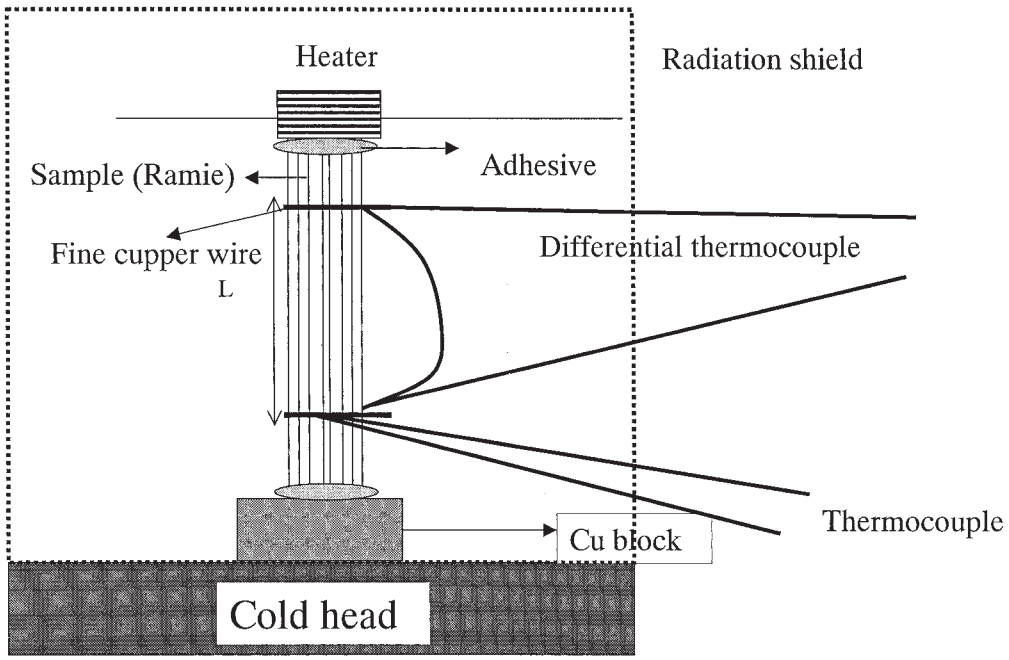


**Figure 2** Schematic diagram of the sample space in the thermal conductivity and diffusivity measurement system with a closed-cycle helium refrigerator.

The fiber samples were stored in a desiccator for more than 3 weeks. The fiber samples were prepared by the bundling f about 6000 monofilaments with a length of 25 mm. Both ends of the fiber bundle were fixed with the adhesive Stycast GT (Emerson & Cuming, Co., Atsugi, Kanagawa, Japan) for uniform cooling and heating among the filaments. One end of the bundle was attached to the cold stage of a GM refrigerator via mechanical pressing with indium metal and the adhesive Stycast GT. A small resistance heater (1 kΩ) was attached to the other end of the bundle with GE7031 varnish (Nilaco, Co., Chuo-ku, Tokyo, Japan). The intermediate positions at which thermocouples were contacted were bound by fine (0.1 mm) Cu wire to keep the temperature uniform in the perpendicular direction of the fibers. The Cu wire and ramie Au (0.07 atom % Fe)–chromel thermocouples were used as thermometers and were attached by GE7031 varnish. The sample space was evacuated below $10^{-3}$ Pa by an oil diffusion pump for heat insulation. A schematic diagram of the sample space in the thermal conductivity measurement system is shown in Figure 2.

The automated measuring system of the thermal conductivity was operated from 10 to 150 K. The measurements were started after the sample space was kept in a high vacuum below $10^{-3}$ Pa for 24 h to dry up the sample. The thermal conductivity was estimated as follows: $\kappa$ (mW/cmK) = $(Q/\Delta T)(L/S)$, where $\kappa$ is the thermal conductivity, $Q$ is the heat flow per second, $\Delta T$ is the temperature difference between thermometers, $L$ is the distance between the thermometers, and $S$ is the cross section of the bundle. The details of the determination of the thermal conductivity are described elsewhere.[18,19]

## Thermal diffusivity

The thermal diffusivity was measured by a nonsteady-state heating method.[18,33] The measurements of the thermal diffusivity were carried out on the same system as that used for the measurements of the thermal conductivity, as shown in Figures 1 and 2. In this method, the time evolutions of the temperature at two measurement points that were intermediate positions between the cold head and 1-kΩ heater were recorded after the application of a heat pulse from the heater, and the measured temperature changes were compared for various thermal diffusivity values via fitting to the one-dimensional diffusion equation $dT/dt = D(d^2T/dx^2)$,[33] where $D$ is the thermal diffusivity, $T$ is the temperature, $t$ is the time, and $x$ is the length in the measured direction. The fiber samples were prepared and were set to the sample space in the same way used for the measurements of the thermal conductivity, as previously mentioned. The sample space was evacuated below $10^{-3}$ Pa by an oil diffusion pump for heat insulation and was kept for 24 h before the measurements for drying up the sample. The automated measuring system of the thermal diffusivity was operated from 10 to 150 K. The details of the determination of the thermal diffusivity are described elsewhere.[18,19]

To measure the water contents of the samples used in the measurements of the thermal conductivity and

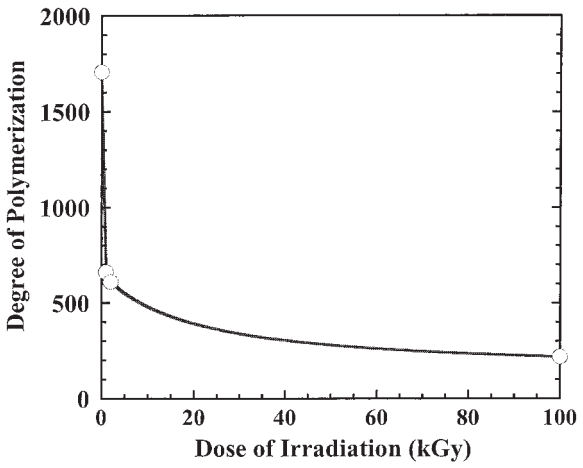


**Figure 3** DP of ramie fibers irradiated with γ rays.

thermal diffusivity, the samples were stored in a high vacuum below $10^{-3}$ Pa for 24 h in the sample space in the same way used for the measurement of the thermal conductivity. The weights of those samples were defined as $W$. The dried samples were obtained by the drying of those samples at 383 K for 8 h in vacuo at 1 Pa, as described elsewhere.[34,35] The weights of the dried samples were defined as $W_d$. The water contents of those samples were estimated by the difference between $W$ and $W_d$.

### Tensile modulus

The tensile test of a single fiber was carried out on a small Tensilon Toyo Sokki UTM-II (Yokohama, Kanagawa, Japan). The span length was 10 mm, and the crosshead speed was 10 mm/min.

## RESULTS AND DISCUSSION

### DP

The DPs of ramie fibers with and without γ-ray treatments, estimated by the measurements of the solution viscosity, are shown in Figure 3. This figure shows that DP of the ramie decreases with irradiation with γ rays. This result shows the main-chain scission of the ramie fiber by the γ-ray treatment. The crystallinity and orientation angle of the ramie fibers with and without the γ-ray treatment are reported in the following section.

### Crystallinity

The CP–MAS, solid-state $^{13}C$ NMR spectrum of ramie fiber is shown in Figure 4. The assignments of the resonance lines are also shown in the figure. The crystal structure of ramie is cellulose I type.[25,36–38] The resonance lines of C4 and C6 carbons split into crystal and amorphous components.[24–26] The peaks of the crystal part are sharp, and those of the amorphous part are broad. The crystallinity can be estimated by the peak separation of those resonance lines. In particular, the peak separation of the C4 resonance is easy because the difference between the crystal peak at 88.8 ppm and the amorphous peak at 83.7 ppm is larger than that of the C6 resonance. Therefore, the C4 resonance peak is used for the estimation of the crystallinity.

First, the solid-state NMR spectra of ramie fibers with and without γ-ray treatments are compared to investigate the changes in the crystal structure by these treatments. The solid-state NMR spectra of ramie fibers with and without γ-ray treatments are shown in Figure 5. The peak assignments are shown in Figure 3. All the NMR spectra show the same peak shape and chemical shifts. This result shows that the crystal structure of the ramie fiber does not change with γ-ray treatments. Comparing the crystal and amorphous resonance peaks of C4 and C6 carbons, we find that the peak intensities do not change so much by γ-ray treatments.

To discuss the crystallinities quantitatively, the C4 resonance peaks are separated into crystal and amorphous peaks. The C4 peak separations of ramie fibers with and without γ-ray treatments are shown in Figure 6. The crystal resonance of the C4 carbon splits into two peaks.[25] As shown in the figure, peak separation of the C4 resonance into crystal and amorphous

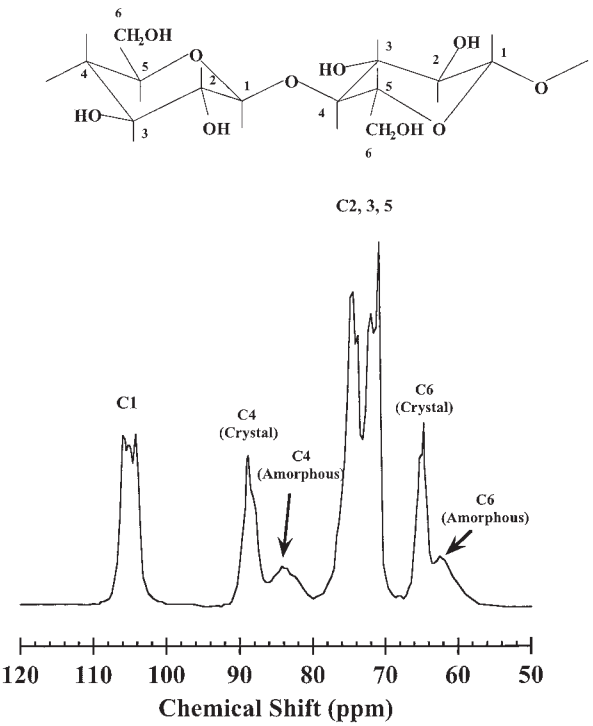


**Figure 4** CP–MAS, solid-state, high-resolution $^{13}C$-NMR spectrum of ramie.

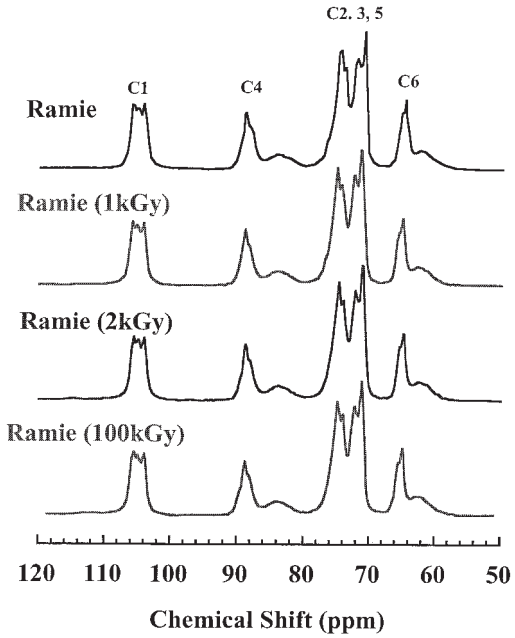


**Figure 5** CP–MAS, solid-state, high-resolution $^{13}$C-NMR spectra of ramie fibers irradiated with $\gamma$ rays.

components is possible. The peak shape and chemical shifts do not change with the $\gamma$-ray treatment as all the spectra shown in Figure 5. The ratio of the crystal peak and amorphous peak does not change so much by the $\gamma$-ray treatment. The crystallinities of those ramie fibers are estimated by the ratio of the area of the peaks separated into crystal and amorphous components quantitatively. The estimated crystallinities are shown in Figure 7. The crystallinity of the ramie fiber does not change with the $\gamma$-ray treatment. Therefore, the thermal conductivity of the ramie fiber is expected to change not so much by the change in the crystallinity with the $\gamma$-ray treatment.

In the following section, the orientation angles of ramie fibers with and without $\gamma$-ray treatments are reported.

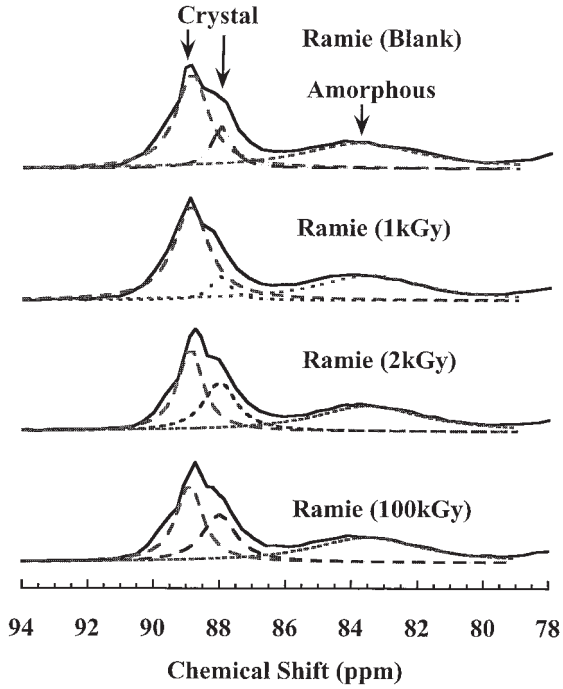


**Figure 6** Line-shape analysis for C4 peaks of ramie cellulose irradiated with $\gamma$ rays in CP–MAS, solid-state $^{13}$C-NMR spectra. The solid lines indicate observed curves, and the broken lines indicate the estimated curves of crystal components and amorphous components.

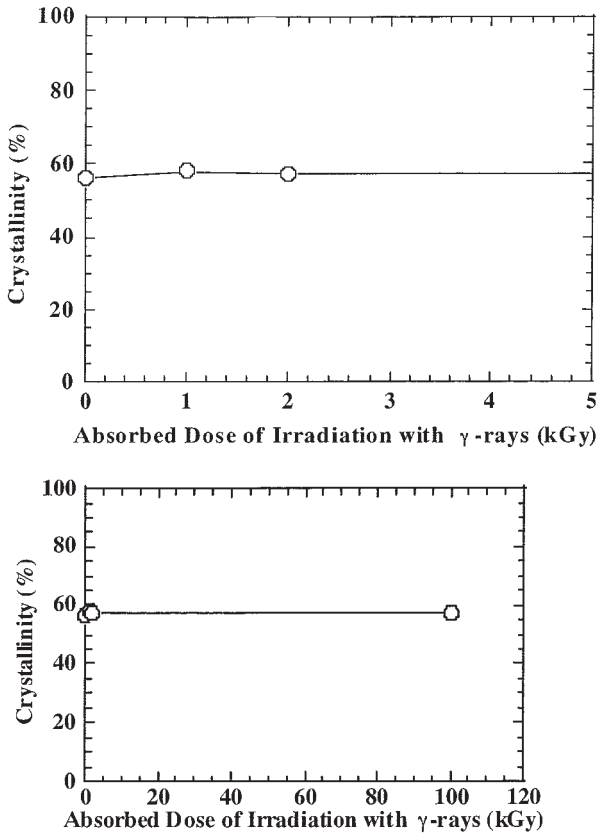


**Figure 7** Relation between the crystallinity and absorbed dose of irradiation with $\gamma$ rays of ramie fibers.

## Orientation angle

The orientation angles of crystals were estimated by the azimuthal intensity distribution of the (002) diffraction spot. X-ray diffraction profiles of the (002) spot of the ramie fibers are shown in Figure 8. This figure shows that the half-width of the diffraction peak changes not so much by $\gamma$-ray treatments. The orientation angles are estimated by the half-width of the diffraction peak, and the orientation degrees are estimated with the orientation angles with the following formula:[28,39]

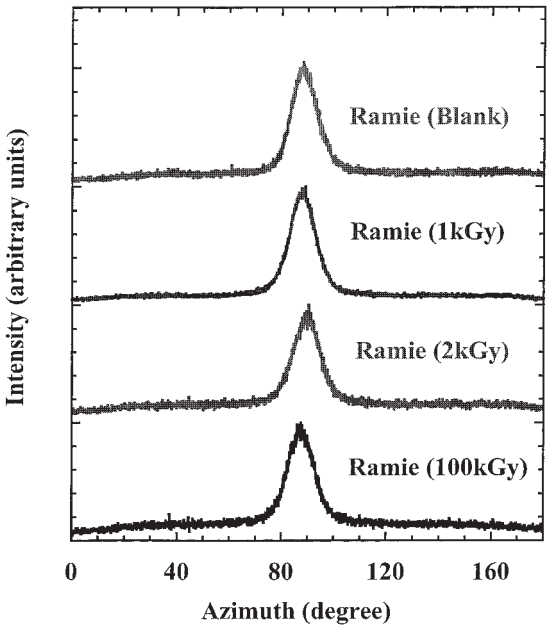


**Figure 8** X-ray diffraction profile of ramie fibers irradiated by γ rays: the azimuthal direction of the (002) spot.

$$\phi = [(180 - \beta)/180] \times 100 \quad (1)$$

where $\phi$ is the orientation degree and $\beta$ is the orientation angle.

The dependence of the orientation angle and orientation degree on the absorbed dose from γ-ray irradiation is shown in Figure 9. The orientation angle and the orientation degree do not change with the γ-ray treatment in the case of an absorbed dose from γ-ray irradiation below 100 kGy.

As previously mentioned, the radiation effects on the DP, crystallinity, and orientation degree by γ rays were investigated. The results are shown in Table I. Those results show that only DP changes and that the crystal structure, crystallinity, and orientation degree do not change with the γ-ray treatment in the case of the ramie fibers used in this work.

## Thermal conductivity

The influence of the thermal radiation effect, fiber bundling, and water in the fibers on the measurement of the thermal conductivity are discussed before the discussion of the change in the thermal conductivity with the γ-ray treatment. The dependence of the observed thermal conductivity on the number of filaments was reported in a previous article.[40] In the temperature range over 200 K, the observed thermal conductivities depend on the number of filaments. It has been inferred to be caused by a thermal radiation effect. Therefore, it is difficult to observe the thermal conductivity at a temperature higher than 200 K with this method. On the other hand, the observed thermal conductivities are independent of the number of filaments in the temperature range below 150 K when the number of filaments is greater than 6000. The independence of the observed thermal conductivity from the number of filaments in the lower temperature range shows that the influence of bundling fibers and thermal radiation can be neglected in this measurement.

The water concentrations of the ramie fibers with and without the γ-ray treatment used in this work are less than 0.1%. The thermal conductivities of the ramie samples before and after a dry treatment at 383 K for 8 h in vacuo at 1 Pa were not different. Therefore, the influence of the thermal conductivity of 0.1% water is neglected in this article. The details are described in a previous article.[40]

The temperature dependence of the thermal conductivity of the ramie fibers with γ-ray treatments in the fiber direction from 10 to 150 K is shown in Figure 10. The thermal conductivities of all the samples decrease with decreasing temperature. Ramie is an electrical insulator. Therefore, it is thought that the thermal conduction of ramie fibers is caused by phonon conduction, like most polymeric materials.

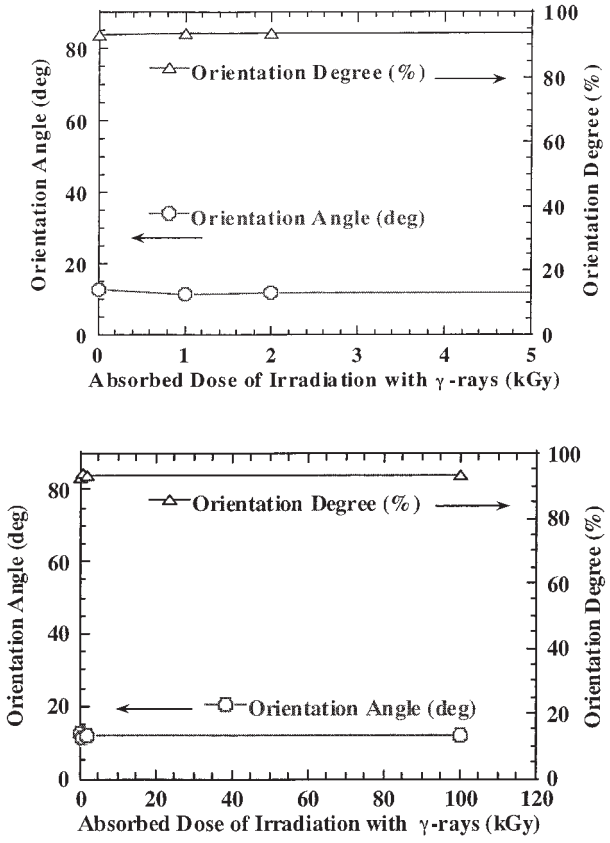


**Figure 9** Dependence of the orientation angle and orientation degree on the absorbed dose of irradiation with γ rays of ramie fibers.

**TABLE I**
**DP, Crystallinity, and Orientation Degree of the Ramie Fibers Irradiated by γ Rays**

| Sample | Absorbed dose of irradiation with γ rays | DP | Crystallinity (%) | Orientation angle (°) | Orientation degree (%) |
|---|---|---|---|---|---|
| Ramie blank | 0 | 1700 | 56 | 12.7 | 92.9 |
| 1 kGy ramie | 1 | 660 | 58 | 11.3 | 93.7 |
| 2 kGy ramie | 2 | 610 | 57 | 11.9 | 93.4 |
| 100 kGy ramie | 100 | 220 | 57 | 11.9 | 93.4 |

We have investigated the effect of the γ-ray treatment on the thermal conductivity. The thermal conductivity of ramie fibers decreases with the γ-ray treatment very much. The reduction of the thermal conductivity is inferred to be caused by the change in the crystallinity, crystal structure, and orientation degree and the reduction of the mean free path of the phonon by chain scission with the γ-ray treatment. However, the crystal structure does not change, and the crystallinity and the orientation degree do not decrease with the γ-ray treatment, as described in the previous sections. Therefore, the reduction of the thermal conductivity by the γ-ray treatment is inferred to be caused by the reduction of the mean free path of the phonon with molecular chain scission.

To clarify the relation between the thermal conductivity and the length of the molecular chain, that is, DP, the relation between the thermal conductivity at 120, 100, 80, and 60 K and DP in the ramie fibers is shown in Figure 11. The DPs of the ramie fibers do not change with cooling. Therefore, the DP values measured at 293 K can be used in the following discussion. As shown in this figure, the thermal conductivity at every temperature decreases with decreasing DP. It is thought that the decrease in the thermal conductivity of ramie by the γ-ray treatment is dominated by the chain scission of molecular chains. To clarify the relation between the thermal conductivity and chain scission, the relation between the thermal conductivity and mean free path of the phonon is discussed in the following. The relation between the thermal conductivity and the mean free path of the phonon is shown in the following formula, and the relation between the thermal diffusivity reported in the following and the mean free path of the phonon is shown in the following formula:[17–19]

$$\kappa = C_p \rho D \tag{2}$$

$$D = (1/3)vl \tag{3}$$

where $\kappa$ is the thermal conductivity in the fiber direction, $C_p$ is the heat capacity at a constant pressure, $\rho$ is the density of the ramie fiber, $D$ is the thermal diffusivity in the fiber direction, $v$ is the sound velocity in the fiber direction, and $l$ is the mean free path of the phonon in the fiber direction. From formulas (2) and (3), the thermal diffusivity of the ramie fiber is also

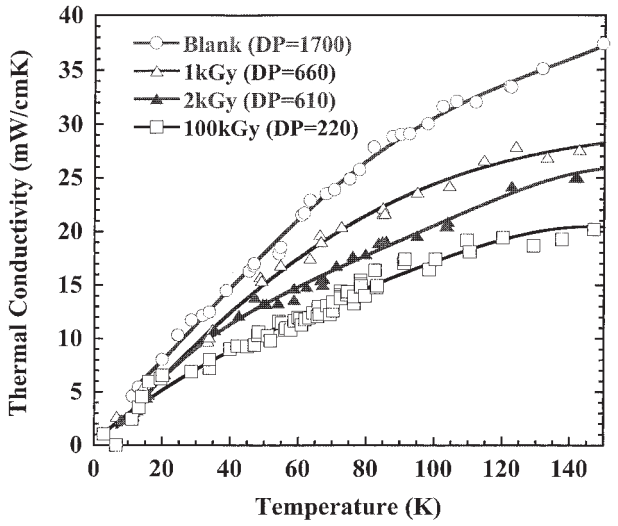


**Figure 10** Temperature dependence of the thermal conductivities of ramie fibers irradiated with γ rays.

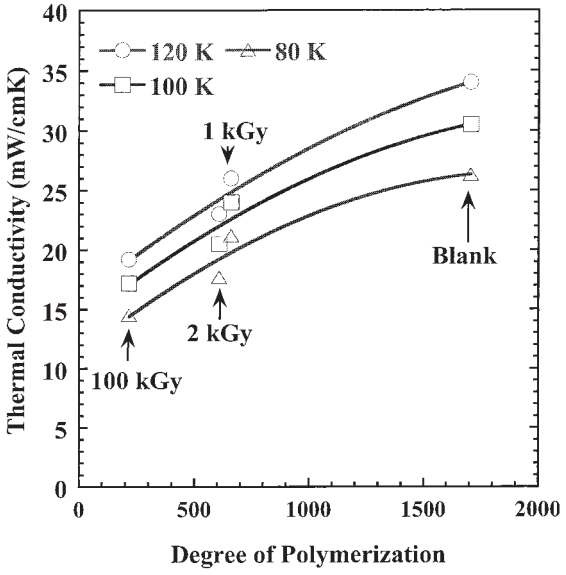


**Figure 11** Relation between the DP and thermal conductivity of ramie fibers irradiated with γ rays.

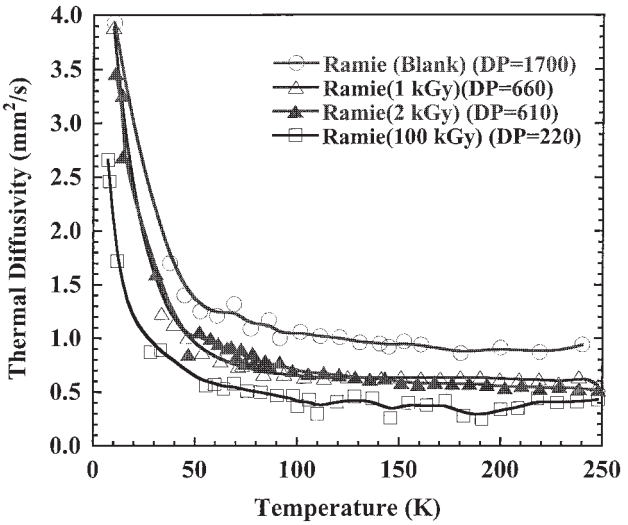


**Figure 12** Temperature dependence of the thermal diffusivities of ramie fibers treated by γ rays.

expected to decrease by the γ-ray treatment, like the thermal conductivity, if the decrease of the thermal conductivity of the ramie fiber by the γ-ray treatment is caused by the reduction of the mean free path of the phonon by molecular chain scission. Therefore, for the certification of this assumption, the thermal diffusivity of the ramie fibers and those with the γ-ray treatment is investigated in the following section.

### Thermal diffusivity

It is reported in a previous article[40] that the behavior of thermal diffusivity is almost independent of the number of measuring filaments. Therefore, the influence of thermal radiation and fiber bundling on the measurement of the thermal diffusivity can be neglected.

The water concentrations in the ramie fibers are less than 0.1%, and the influence of the water on the thermal conductivity can be neglected, as previously mentioned. The change in the heat capacity by 0.1% water has been estimated to be about 0.25% according to the relation between the heat capacity and water contents.[41] Therefore, it is also thought that the change in the thermal diffusivity by 0.1% water can be neglected according to formula (2).

The temperature dependence of the thermal diffusivities in the fiber direction of ramie fibers with and without the γ-ray treatment is shown in Figure 12. The thermal diffusivities of all the ramie fibers are almost constant from 250 to 100 K, increase slightly as the temperature decreases from 100 to 50 K, and increase rapidly as the temperature decreases below 50 K. The phonons are scattered by the end of the molecular chain, the crystal or amorphous boundary, and defects. Therefore, the mean free path of the phonon is determined by those concentrations in this temperature range.[15] Those concentrations of the end of the molecular chain, crystal or amorphous boundary, and defects are independent of the temperature. Almost temperature-independent thermal diffusivity has been reported about other amorphous and crystal polymers.[15,42] On the other hand, increasing the thermal diffusivity via cooling below 50 K is considered to be due to the mean free path of the phonon increasing with decreasing phonon scattering. Increasing the thermal diffusivity by cooling is considered to be caused by two factors. One is the increasing sound velocity with increasing tensile modulus of the amorphous region by cooling. The other is the increasing phonon mean free path with decreasing phonon scattering caused by decreasing lattice vibration at a low temperature. In this case, it is not thought that the tensile modulus increases rapidly below 50 K, like the glass transition.

The change in the thermal diffusivity by the γ-ray treatment is investigated in the following. The thermal diffusivity from 250 to 50 K decreases with the γ-ray treatment, like the thermal conductivity. With the results in the previous section, it is thought that decreasing thermal diffusivity is caused by the reduction of the phonon mean free path by the molecular chain scission with the irradiation of γ rays. To clarify the relation between the molecular chain length and thermal diffusivity of ramie, the relation between the thermal diffusivity at 240 K and DP is shown in Figure 13. The thermal diffusivity of ramie at 240 K decreases with increasing absorbed dose from γ-ray irradiation. The thermal diffusivities of ramie (1 kGy) and ramie (2 kGy) are not so different. The DPs of ramie (1 kGy)

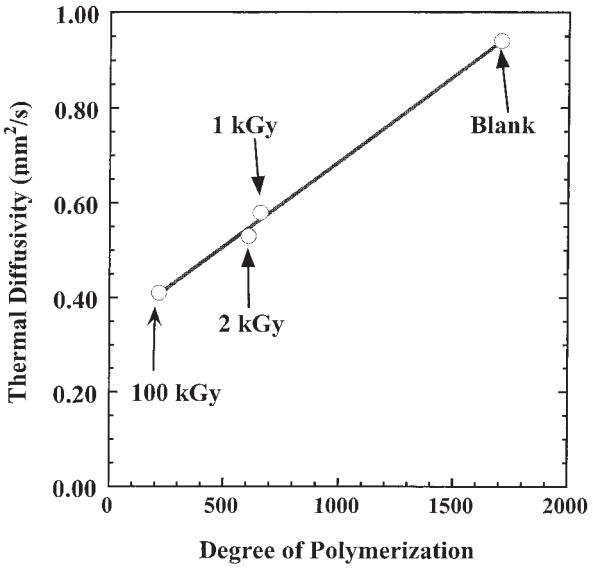


**Figure 13** Relation between the thermal diffusivity at 240 K and DP of ramie fibers treated by γ rays.

and ramie (2 kGy) are 610 and 660, respectively. These are also not so different. The small difference in the thermal diffusivities is inferred to be due to the small difference in the DPs, that is, the small difference in the average length of the molecular chain between ramie (1 kGy) and ramie (2 kGy). The reduction of the thermal diffusivity of the ramie fiber by the γ-ray treatment agrees with the reduction of DP. This reduction of the thermal diffusivity with the reduction of DP agrees with that of thermal conductivity mostly.

Next, the change in the mean free path of the phonon by the γ-ray treatment is investigated. The crystal region and amorphous region are mixed in the ramie fiber used in this work. The mean free path of the phonon in the crystal region and that in the amorphous region are different. Therefore, it is difficult to discuss the absolute value of the phonon mean free path in the crystal region in this work, so the relative change in the average behavior of the phonon mean free path in the mixture of crystal and amorphous parts by molecular chain scission by the γ-ray treatment is discussed in this work. The tensile modulus in the fiber direction of the ramie fiber is 61 GPa. The tensile moduli of ramie (1 kGy), ramie (2 kGy), and ramie (100 kGy) are 55, 53, and 69 GPa, respectively. The densities of those samples are 1.54 g/cm$^3$. The sound velocity in the fiber direction is estimated with the tensile modulus and density with the following formula:

$$v = (E/\rho)^{1/2} \tag{4}$$

where $v$ is the sound velocity, $E$ is the tensile modulus, and $\rho$ is the density of ramie.

By the substitution of the numerical values of $E$ and $\rho$ into formula (4), the sound velocities of ramie (blank), ramie (1 kGy), ramie (2 kGy), and ramie (100 kGy) have been estimated to be 6400, 5000, 5900, and 6800 m/s, respectively. The thermal diffusivities of those ramie fibers show almost constant values from 50 to 250 K, as shown in Figure 12. Therefore, the thermal diffusivities of the ramie fibers at room temperature are expected to be equal to those at 240 K. The mean free path of the phonon in the ramie fibers with the γ-ray treatment can be compared with that in the blank ramie fiber relatively with formula (3) and the sound velocity estimated by formula (4) under the assumption that the thermal diffusivities at room temperature are equal to those at 240 K. The relative dependence of the phonon mean free path on DP is shown in Figure 14. The mean free path of the phonon decreases with decreasing DP. It is inferred that the thermal diffusivity and thermal conductivity decrease with the reduction of the phonon mean free path by molecular chain scission with the irradiation of γ rays.

The reduction of the thermal conductivity, thermal diffusivity, and phonon mean free path by the γ-ray treatment is smaller than that of DP. It is thought that the probability of molecular chain scission by the γ-ray treatment in the crystal region is different from that in the amorphous region and that the molecular chain scission in the amorphous region contributes to the change in the thermal conductivity not so much in comparison with that in the crystal region. A more detailed discussion including structural analysis will be necessary for the quantitative discussion of the relation between the thermal conductivity and γ-ray treatment.

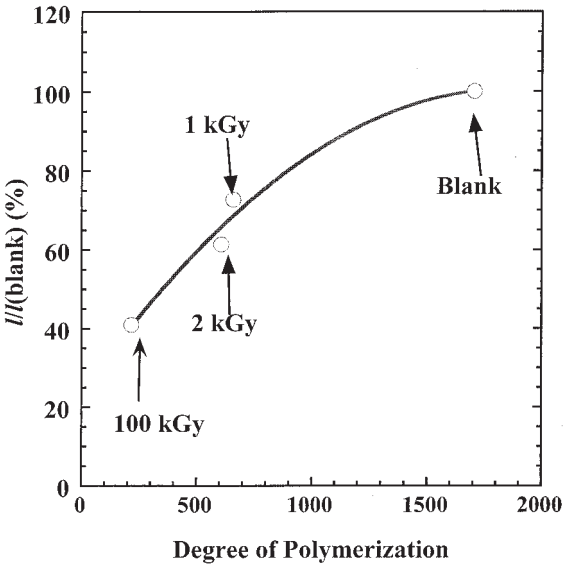


**Figure 14** Relation between the ratio of the phonon mean free path in the fiber direction of ramie fibers treated by γ rays to that of blank ramie fiber [$l/l$(blank)] and DP.

Next, the change in the thermal diffusivity by molecular chain scission by the γ-ray treatment at a low temperature is investigated. As previously mentioned, the thermal diffusivities of all the ramie samples increase with cooling. The thermal diffusivities increase slightly with the temperature decreasing from 100 to 50 K and increase rapidly with the temperature decreasing below 50 K. To compare the temperature dependence of the thermal diffusivity, the thermal diffusivities divided by that at 240 K from 250 to 10 K are shown in Figure 15. Those are relative values to the thermal diffusivity at 240 K. All the curves show almost the same behavior. That is, the temperature dependence of the thermal diffusivities of all the samples shows similar behavior, although the thermal diffusivity values of the ramie fibers are different, as shown in Figures 12 and 13. Therefore, it is thought that only the change in the phonon mean free path influences the thermal diffusivity of the ramie fiber at all temperature in the case of molecular chain scission by radiation.

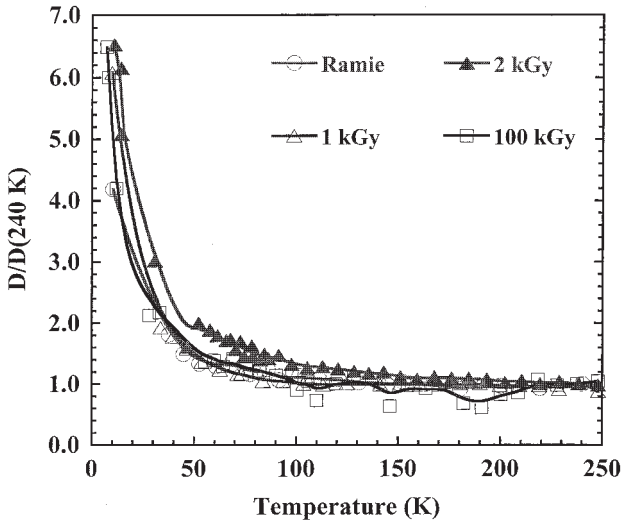


**Figure 15** Temperature dependence of $D/D(240\ K)$ of ramie fibers treated with γ rays. $D$ is the thermal diffusivity, and $D(240\ K)$ is the thermal diffusivity at 240 K.

## CONCLUSIONS

The thermal conductivity, thermal diffusivity, fiber structure, and DP were measured for ramie fibers and those irradiated by γ rays, for which the absorbed doses were 1, 2, and 100 kGy [ramie (1 kGy), ramie (2 kGy), and ramie (100 kGy), respectively]. The effects of molecular chain scission with radiation on the thermal conductivity and thermal diffusivity were investigated. The following conclusions were drawn:

1. Only DP decreased with the γ-ray treatment (the absorbed doses were 1, 2, and 100 kGy). The crystal structure, crystallinity, and orientation degree did not change with the γ-ray treatment. The molecular chain scission of the ramie fiber by γ rays was estimated by the change in DP.
2. The thermal conductivities of the ramie fibers and those with γ-ray treatments decreased with decreasing temperature.
3. The thermal conductivity of the ramie fibers decreased with increasing absorbed from γ-ray irradiation. The reduction of the thermal conductivity of the ramie fibers by the γ-ray treatment agreed with the reduction of DP.
4. The thermal diffusivities of the ramie fibers with and without γ-ray treatments were almost constant from 250 to 100 K, increased with the temperature decreasing from 100 to 50 K, and increased very much with the temperature decreasing below 50 K.
5. The thermal diffusivity of the ramie at 240 K decreased with increasing absorbed dose from γ-ray irradiation. The reduction of the thermal diffusivity of the ramie fiber by the γ-ray treatment agreed with the reduction of DP.
6. The mean free path of the phonon in ramie was reduced by the γ-ray treatment. From those results, the reduction of the thermal conductivity and thermal diffusivity was explained by the reduction of the phonon mean free path by molecular chain scission.
7. The temperature dependence of the thermal diffusivities of the ramie fibers with and without the γ-ray treatment showed similar behavior at a low temperature.

As previously mentioned, the thermal conductivity and thermal diffusivity decreased with a reduction of the mean free path of the phonon by molecular chain scission with the γ-ray treatment, although the crystallinity and orientation degree did not decrease. Those results suggest that the thermal conductivity of polymeric fibers can be controlled by the control of the length of the molecular chain.

Many thanks are due to Mr. Atsushi Hamai (Fiber Business Unit, Toyobo) for obtaining ramie samples. The authors' gratitude is also expressed to Dr. Fumitaka Horii (Professor of Kyoto University), Dr. Seichi Ochi (Research and Development Department, Toyobo), Dr. Masao Murano (Professor of Saga University), and Dr. Atsushi Kaji as well as Dr. Yuji Shimizu (Toyobo) for their valuable advice and references with respect to cellulose and its structural analysis. Thanks are also due to Dr. Hiroshige Sugiyama and Dr. Sonoko Ishimaru (Toyobo) for their advice and references on the engineering applications of thermal conductivity. The authors express their appreciation to Ms. Sayuri Nagao (Toyobo) and Mr. N. Nakajima (JEMS Co.), who were very helpful with the experiments. They also thank Manabu Ikebe (Professor of Iwate University), Dr. Hiroshi Hirahata, Dr. Yukihiro Nomura, and the members of their group (Toyobo Functional Fiber Group), and Mr. Toshiyuki Matsui (manager), Tokuichi Maeda, and other members of the Toyobo Dyneema Division, in addition to Dr. Takaharu Ichiryu (Zylon Business Unit), Dr. Keiji Yukimatsu (President of Nippon Dyneema), and Dr. Masatoshi Yoshikawa (Textiles Products Development Center, Toyobo) for their support.

## References

1. Yoneda, M.; Kawabata, S. J Text Machinery S Jpn 1981, 34, 183.
2. Yoneda, M. J Text Machinery S Jpn 1982, 35, 365.
3. Kawabata, S. J Text Machinery S Jpn 1984, 37, 131.
4. Nishijima, S.; Okada, T.; Niihara, K. Key Eng Mater 1999, 161, 535.
5. Hand Book of Superconductivity and Cryogenic Engineering; Cryogenic Association of Japan: Oumusha, Japan, 1993.
6. Takao, T.; Kawasaki, A.; Yamaguchi, M.; Yamamoto, H.; Niiro, A.; Nakamura, K.; Yamanaka, A. IEEE Trans Appl Supercond 2002, 13, 1776.
7. Agari, Y.; Kamiyama, T. Plastics 2003, 54, 49.
8. Bhowmick, T.; Pattanayak, S. Cryogenics 1990, 30, 116.
9. Jackel, M.; Muller, M.; Claverie, A. L.; Arndt, K. F. Cryogenics 1991, 31, 228.

10. Choy, C. L.; Wong, S. P.; Young, K. J Polym Sci Polym Phys Ed 1985, 23, 1495.
11. Choy, C. L.; Leung, W. P. J Polym Sci Polym Phys Ed 1983, 21, 1243.
12. Mergenthaler, D. B.; Pietralla, M.; Roy, S.; Killian, H. G. Macromolecules 1992, 25, 3500.
13. Burgress, S.; Greig, D. J Phys C: Solid State Phys 1975, 8, 1637.
14. Gibson, A. G.; Greig, D.; Sahota, M.; Ward, I. M.; Choy, C. L. J Polym Sci Polym Lett Ed 1977, 15, 183.
15. Choy, C. L. Polymer 1977, 18, 984.
16. Choy, C. L.; Luk, W. H.; Chen, F. C. Polymer 1978, 19, 155.
17. Yamanaka, A.; Fujishiro, H.; Kashima, T.; Kitagawa, T.; Ema, K.; Izumi, Y.; Nishijima, S. J Polym Sci Part B: Polym Phys 2005, 43, 1495.
18. Fujishiro, H.; Ikebe, M.; Kashima, T.; Yamanaka, A. Jpn J Appl Phys 1997, 36, 5633.
19. Fujishiro, H.; Ikebe, M.; Kashima, T.; Yamanaka, A. Jpn J Appl Phys 1998, 37, 1994.
20. Kittel, C. Introduction to Solid State Physics; Academic: New York, 1974.
21. Phillips, G. O.; Arthur, J. C., Jr. In Cellulose Chemistry and Its Applications; Nevell, T. P.; Zeronian, S. H., Eds.; Wiley: New York, 1985; Chapter 12, p 290.
22. Cyclopedia of Cellulose; Cellulose Society Japan, Ed.; Academic: Asakura Shoten, Japan, 2000.
23. Klemm, D.; Philipp, B.; Heinze, T.; Heinze, U. Comprehensive Cellulose Chemistry; Wiley-VCH: Weinheim, 1998; Chapter 1, p 168.
24. VanderHart, D. L.; Atalla, R. H. Macromolecules 1984, 17, 1465.
25. Horii, F. In Nuclear Magnetic Resonance in Agriculture; Pfeffer, P. E.; Gerasimowicz, W. V., Eds.; CRC: Boca Raton, FL, 1989; Chapter 10, p 311.
26. Horii, F.; Hirai, A.; Kitamaru, R. Polym Bull 1982, 8, 163.
27. Sakaguchi, Y.; Tsutsumi, M.; Kaji, A.; Abe, S. Senni-Gakkaishi 2002, 58, 321.
28. Abe, S.; Tsutsumi, M.; Yoshikawa, M.; Sakaguchi, Y. J Text Machinery S Jpn 2000, 53, 1.
29. Dudley, R. L.; Fyfe, C. A.; Stephenson, P. J.; Deslandes, Y.; Hamer, G. K.; Marchessaulft, R. H. J Am Chem Soc 1983, 105, 2469.
30. Horii, F.; Hirai, A.; Kitamaru, R. Macromolecules 1987, 20, 2117.
31. Yamato, H.; Horii, F.; Odani, H. Macromolecules 1989, 22, 4130.
32. Abe, S.; Ohta, S.; Yamanaka, A.; Nagara, N. J Text Machinery S Jpn 1996, 49, 290.
33. Fujishiro, H.; Ikebe, M.; Naito, T.; Noto, K. Cryog Eng 1993, 28, 533.
34. Wada, M.; Heux, L.; Isogai, A.; Nishiyama, Y.; Chanzy, H.; Sugiyama, J. Macromolecules 2001, 34, 1237.
35. Miyake, H.; Nagura, M. Text Res J 2001, 71, 645.
36. Woodcock, C.; Sarko, A. Macromolecules 1980, 13, 1183.
37. Ishikawa, A.; Sugiyama, J.; Okano, T. Wood Res 1994, 81, 16.
38. Earl, W. L.; VanderHart, D. L. Macromolecules 1981, 14, 570.
39. Abe, S.; Ohta, S.; Tsutsumi, M. J Text Machinery S Jpn 1997, 50, 109.
40. Yamanaka, A.; Yoshikawa, M.; Abe, S.; Tsutsumi, M.; Oohazama, T.; Kitagawa, T.; Fujishiro, H.; Ema, K.; Izumi, Y.; Nishijima, S. J Polym Sci Part B: Polym Phys 2005, 43, 2754.
41. Hatakeyama, H.; Hatakeyama, T. Thermochim Acta 1998, 308, 3.
42. Morikawa, J.; Tan, J.; Hashimoto, T. Polymer 1995, 36, 4439.